

Figure 10 Simulation result and measurement result

9 shows the photograph of the filter, the full size is less than  $6.5 \text{ mm} \times 6.5 \text{ mm} \times 1.3 \text{ mm}$ . The filter is measured in Agilent's PNA 8363B. The  $K$  connector is used to connect the filter and the PNA 8363B. The simulation result and measurement result are shown in Figure 10. The insertion loss is 3.1 dB at the central frequency 9.75 GHz, and the relative bandwidth is 5%. The suppression at 8.4 and 10.8 GHz reaches to 35 dB, and there is a transmission zero at 11.0 GHz where the suppression reaches to 60 dB. Comparing the simulation result, the measured central frequency goes higher from 9.6 to 9.75 GHz, the insertion loss deteriorates from 2.1 to 3.1 dB. The frequency deviation is due to the deviation of the permittivity of LTCC substrate. The permittivity, 5.9, is used in 3D-simulation and the real permittivity may be 5.7 or less. The larger insertion loss in measurement due to the metal loss which is ignored in the 3D simulation, at the same time, the size of the CPW input/output is too small for the  $K$  connector to connect well with the filter, thus the  $K$  connector between the filter and the PNA 8363B also introduces large loss and reflection in the measurement.

#### 4. CONCLUSION

A very compact combline filter of X-band is designed, fabricated, and measured in LTCC. The simulated and measured responses agree with each other well. In the filter, the lumped capacitance in traditional combline filter is replaced by coupled stripline in LTCC layers. The compact filter achieves a small size less than  $6.5 \text{ mm} \times 6.5 \text{ mm} \times 1.3 \text{ mm}$  while having very good suppression performance out of pass band. The filter can be used in modern radar system and can miniaturize the system effectively.

#### REFERENCES

1. L.K. Yeng and K.-L. Wu, A compact second-order LTCC bandpass filter with two finite transmission zeros, *IEEE Trans Microwave Theory Tech* 51 (2003), 337–341.
2. A. Simine and D. Kholodnyak, Enhancement of inductance Q-factor for LTCC filter design, 2005 European Microwave Conference, Vol. 2, 4–6 Oct. 2005.
3. G. Wang, M. Van, F. Barlow, and A. Elshabini, An interdigital bandpass filter embedded in LTCC for 5-GHz wireless LAN applications, *IEEE Microwave Wireless Compon Lett* 15 (2005), 357–359.
4. Y. Hee Cho, D. Yun Jung, Y. Chul Lee, J.W. Lee, M. Sun Song, E.-S. Nam, S. Kang, and C. Soon Park, A fully embedded LTCC multilayer BPF for 3D integration of 40-GHz, *IEEE Trans Adv Packag* 30 (2007), 521–525.
5. G.L. Matthaci, L. Young, E.M.T. Jones. *Microwave filters, impedance*

matching networks and coupling structures, McGraw-Hill, New York, 1964.

6. S. Caspi and J. Adelman, Design of combline and interdigital filters with tapped-line input, *IEEE Trans Microwave Theory Tech* 36 (1988), 759–763.
7. R. Levy, H.-W. Yao, and K.A. Zaki, Transitional combline/evanescent-mode microwave filters. *IEEE Trans Microwave Theory Tech* 45 (1997), 2094–2099.
8. J.-S. Hong and M.J. Lancaster, *Microstrip filter for RF/microwave applications*, Wiley, New York, NY, 2001.

© 2008 Wiley Periodicals, Inc.

## BROADBAND PLANAR DIPOLE ANTENNA FOR DTV/GSM OPERATION

Cheng-Tse Lee and Kin-Lu Wong

Department of Electrical Engineering, National Sun Yat-Sen University, Kaohsiung 804, Taiwan; Corresponding author: leect@ema.ee.nsysu.edu.tw

Received 12 November 2007

**ABSTRACT:** This article presents a new broadband planar dipole antenna for DTV signal reception in the UHF band (470 ~ 862 MHz) and mobile communications in the GSM850/900 band (824 ~ 894/890 ~ 960 MHz), which requires an operating bandwidth (3:1 VSWR) of 490 MHz or about 69% centered at 715 MHz. The antenna has two radiating arms (arm 1 and arm 2) with a total length 230 mm and a width 14 mm, which are easily printed on an FR4 substrate. Broadband operation is obtained from successful excitation of the half- and one-wavelength modes of the antenna, which is achieved by shifting the antenna's feeding point away from the dipole center through adding a tuning strip to arm 1 and embedding a tuning slot to arm 2. The tuning strip is extended across the tuning slot, and both are also formed as an internal matching circuit for achieving good impedance matching of the excited half- and one-wavelength modes of the antenna. The proposed antenna is presented and studied. © 2008 Wiley Periodicals, Inc. *Microwave Opt Technol Lett* 50: 1900–1905, 2008; Published online in Wiley InterScience (www.interscience.wiley.com). DOI 10.1002/mop.23500

**Key words:** printed dipole antennas; broadband antennas; DTV antennas; planar antennas; GSM operation

#### 1. INTRODUCTION

Some promising designs of the broadband planar dipole antenna suitable for DTV (Digital Television) signal reception in the UHF band has recently been reported [1–3]. This kind of planar dipole antenna is easy to fabricate by printing on a thin dielectric substrate and is very suitable to be attached horizontally along the edge of the window pane of a vehicle to achieve an aesthetical appearance. With the horizontal arrangement, the dipole antenna is especially suitable for receiving horizontally polarized DTV signals [4, 5].

In this article, we present another promising broadband planar dipole antenna suitable not only for DTV reception in the 470 ~ 862 MHz band covering the European DVB-H band [6] or the 470 ~ 806 MHz band (channels 14–69 [7]), but also for mobile communications in the GSM850/900 band (824 ~ 894/890 ~ 960 MHz) [8]. Broadband operation of the proposed dipole antenna is obtained by successfully exciting its half- and one-wavelength modes, which are further adjusted to be at close frequencies to form a wide operating band for DTV/GSM operation. The operation concept of the proposed antenna using two adjacent resonant modes is different from that of using two separate resonant modes

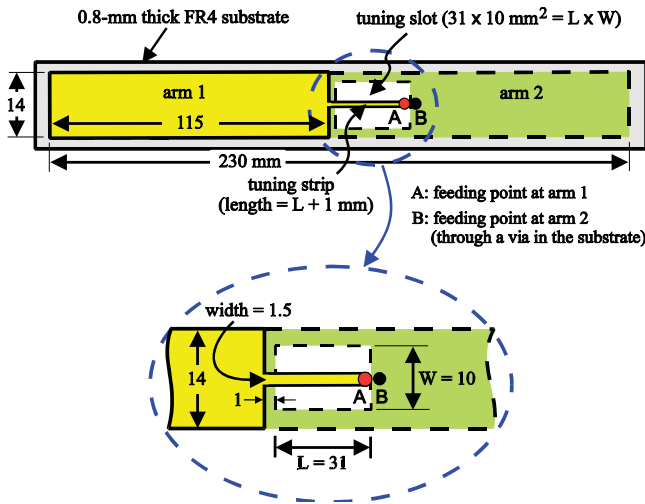


**Figure 1** Geometry of the proposed broadband planar dipole antenna for DTV/GSM operation. [Color figure can be viewed in the online issue, which is available at [www.interscience.wiley.com](http://www.interscience.wiley.com)]

(both are half-wavelength modes) excited in the reported dipole antenna with two U-slotted arms or two L-slotted arms for dual-band operation [9], [10]. For the obtained bandwidth of the proposed antenna, it is generally larger than those of the reported planar DTV antennas for mobile devices [1-5, 11-14]. Detailed design considerations of achieving broadband operation for the proposed antenna are described in the article. Radiation characteristics over the operating band of the antenna are also studied.

## 2. DESIGN CONSIDERATIONS OF PROPOSED ANTENNA

Figure 1 shows the geometry of the proposed broadband planar dipole antenna for DTV/GSM operation. The antenna is printed on a thin (0.8-mm thick) FR4 substrate and comprises two radiating arms (arm 1 and arm 2) with a total length 230 mm and a width 14 mm. Arm 1 and arm 2 are generally of the same length 115 mm and are extended in opposite directions. Notice that arm 1 is printed on the front surface of the substrate and arm 2 is on the back surface. The total length of the antenna is close to about one-half wavelength at 550 MHz, thus allowing the antenna to generate a half-wavelength mode to cover the lower frequency portion of the desired operating band.

To successfully excite the one-wavelength mode to cover the higher frequency portion of the desired operating band, the feeding points of the antenna (point A at arm 1 and point B at arm 2) are moved away from the dipole center. In this case, it is possible that the large input impedance of the one-wavelength mode be greatly decreased, while that of the half-wavelength mode is slightly affected. For this purpose, a narrow (width 1.5 mm) tuning strip of proper length is connected to arm 1 at the dipole center; hence, point A now at the open end of the tuning strip is moved away from the dipole center. At the same time, a tuning slot of length  $L$  (31 mm here) and width  $W$  (10 mm here) is embedded in arm 2 near the dipole center and is also centered below the tuning strip; notice that the length  $(L + 1 \text{ mm})$  of the tuning strip is related to the length  $(L)$  of the tuning slot. The tuning slot makes the feeding point B at arm 2 to be moved away from the dipole center. In addition, both the tuning strip and the tuning slot are formed into an internal matching circuit for the antenna. The tuning strip contributes an additional inductance to the antenna's input impedance, and by adjusting its length  $(L + 1 \text{ mm})$  here, the contributed inductance can be adjusted. On the other hand, by varying the size

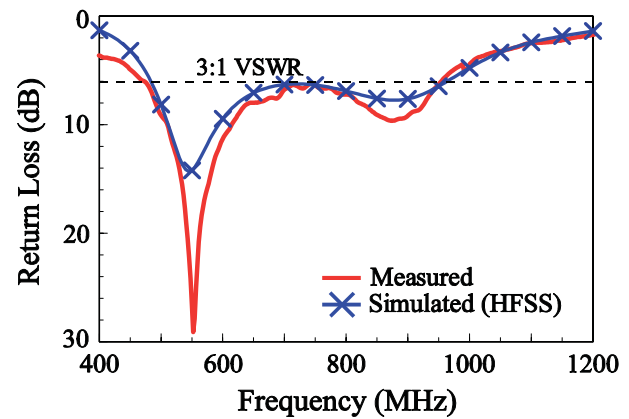


**Figure 2** Measured and simulated return loss for the proposed antenna. [Color figure can be viewed in the online issue, which is available at [www.interscience.wiley.com](http://www.interscience.wiley.com)]

$(L \times W)$  of the tuning slot, the capacitive coupling between the tuning strip and arm 2 is varied; hence there is a contributed capacitance controlled by the size of the tuning slot. Thus, with proper dimensions of the tuning strip and the tuning slot chosen, good impedance matching over the whole desired operating band can be achieved.

It is also noted that, owing to the contributed inductance of the narrow tuning strip, the half-wavelength mode of the antenna is shifted to lower frequencies; that is, the proposed antenna has a reduced length for operating at the same frequency as compared to the conventional center-fed dipole antenna. This behavior is mainly because the additional inductance can lead to the additional phase added to the excited current. This is equivalent to an increase in the effective electrical length of the proposed antenna. Hence, the fundamental (half-wavelength) resonant mode of the antenna can be shifted to lower frequencies. Also note that, for testing the antenna in the experiment, a 50- $\Omega$  mini coaxial line (not shown in the figure) is used, whose central conductor and outer grounding sheath are connected to point A and point B, respectively, or vice versa. In addition, in order to eliminate the possible unbalanced surface currents flowing back from the dipole antenna to the coaxial line to affect the measurement in the experiment, a balun element is added in between the feeding points (points A and B) and the coaxial line.

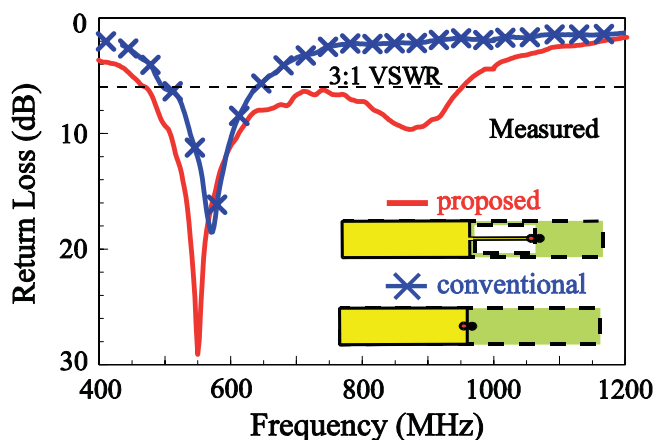


**Figure 3** Measured return loss for the proposed antenna and the corresponding conventional planar dipole antenna. [Color figure can be viewed in the online issue, which is available at [www.interscience.wiley.com](http://www.interscience.wiley.com)]

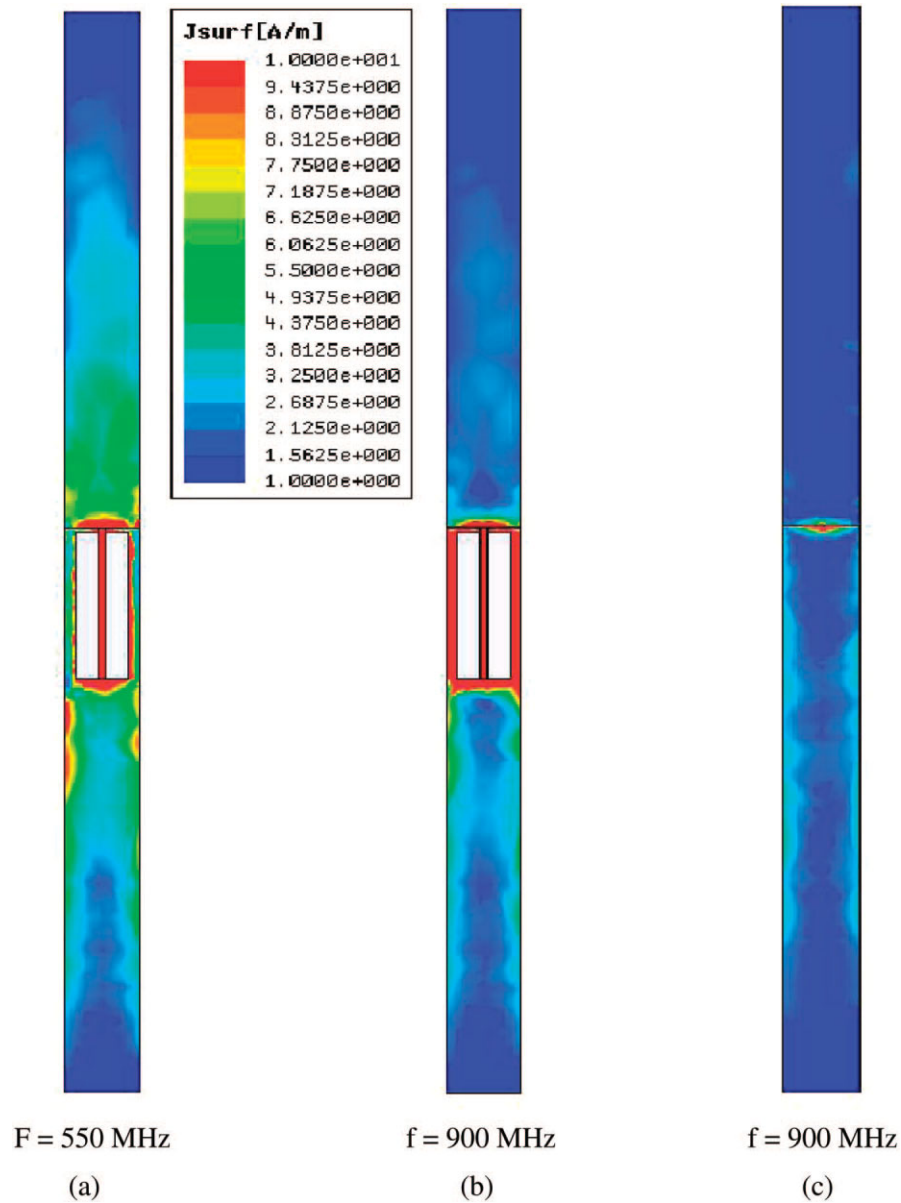


**Figure 4** Simulated excited surface current distributions. (a) The proposed antenna at 550 MHz. (b) The proposed antenna at 900 MHz. (c) The conventional planar dipole antenna at 900 MHz. [Color figure can be viewed in the online issue, which is available at [www.interscience.wiley.com](http://www.interscience.wiley.com)]

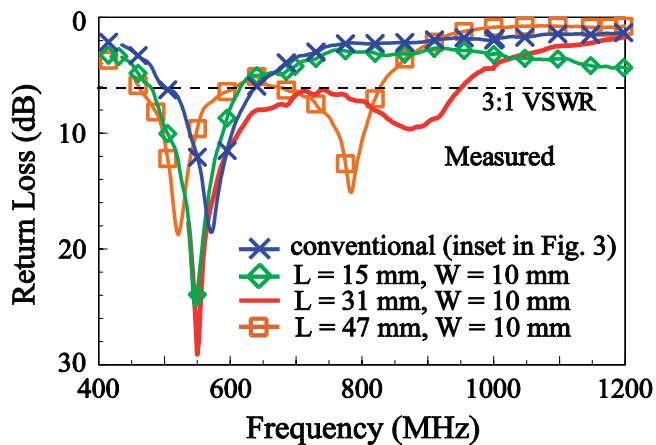


**Figure 5** Measured return loss as a function of  $L$ ; other dimensions are the same as in Fig. 1. [Color figure can be viewed in the online issue, which is available at [www.interscience.wiley.com](http://www.interscience.wiley.com)]

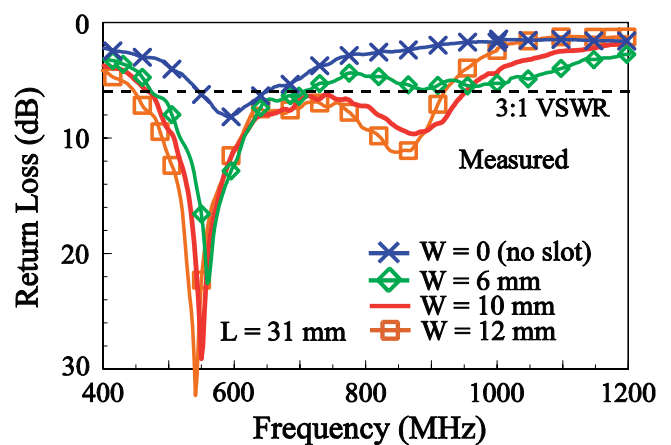


**Figure 6** Measured return loss as a function of  $W$ ; other dimensions are the same as in Fig. 1. [Color figure can be viewed in the online issue, which is available at [www.interscience.wiley.com](http://www.interscience.wiley.com)]

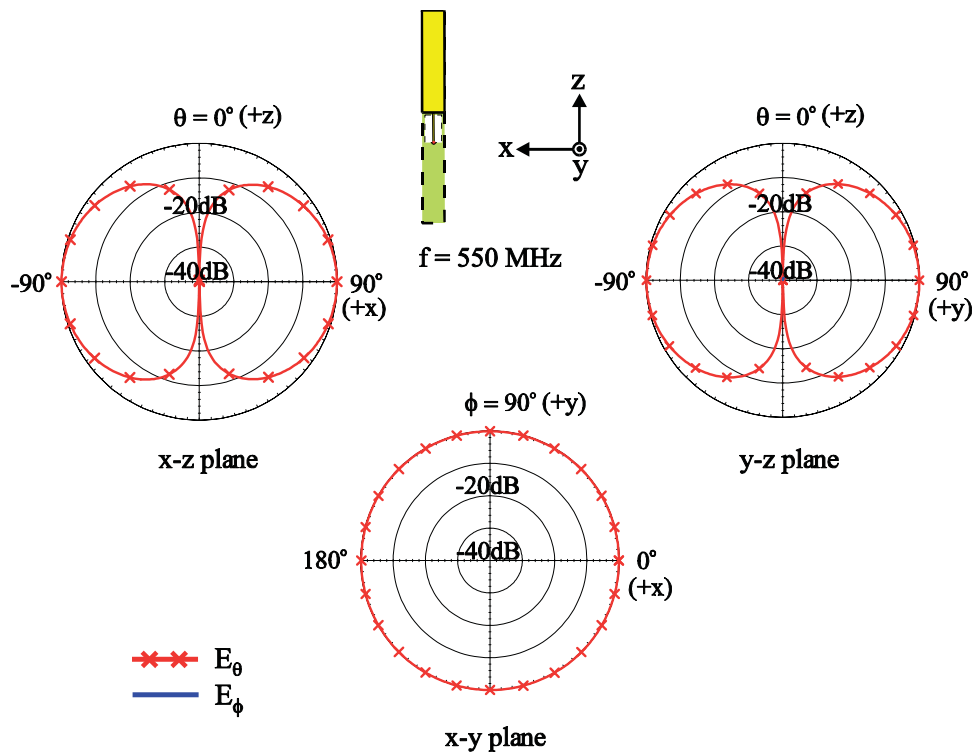


**Figure 7** Measured radiation patterns at 550 MHz for the proposed antenna. [Color figure can be viewed in the online issue, which is available at [www.interscience.wiley.com](http://www.interscience.wiley.com)]

### 3. RESULTS AND DISCUSSION

Figure 2 shows the measured and simulated return loss for the proposed antenna. The simulated results are obtained using Ansoft HFSS (High Frequency Structure Simulator) [15], and good agree-

ment between the measured data and simulated results are obtained. Results clearly show that two resonant modes are excited at about 550 and 900 MHz and formed into a wide operating band. With the bandwidth definition of 3:1 VSWR (6 dB return loss),

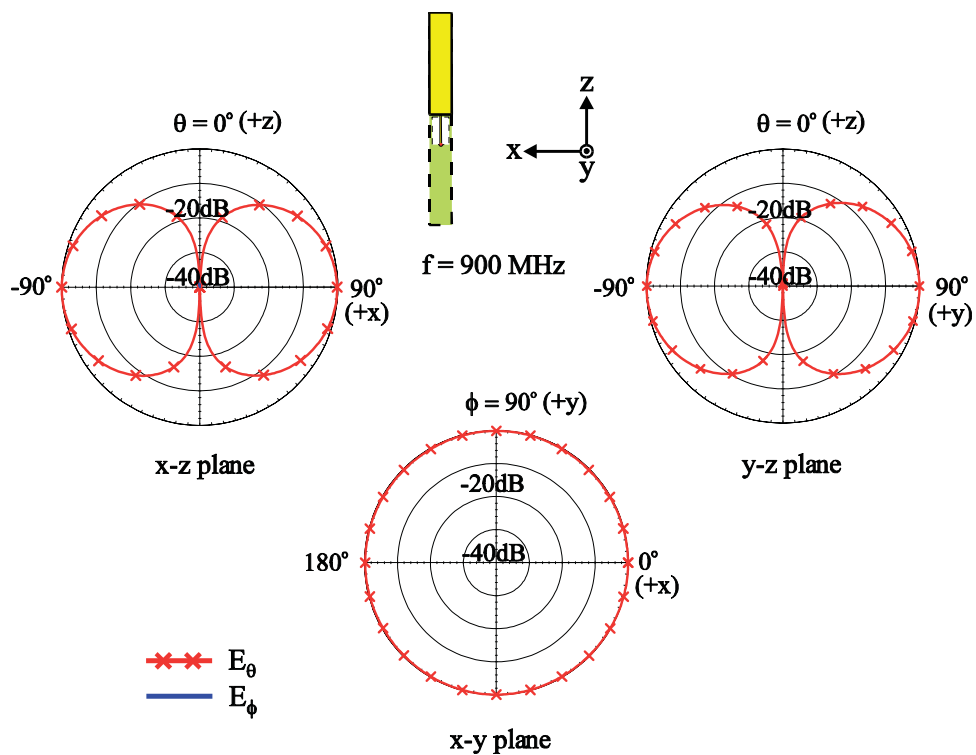


**Figure 8** Measured radiation patterns at 900 MHz for the proposed antenna. [Color figure can be viewed in the online issue, which is available at [www.interscience.wiley.com](http://www.interscience.wiley.com)]



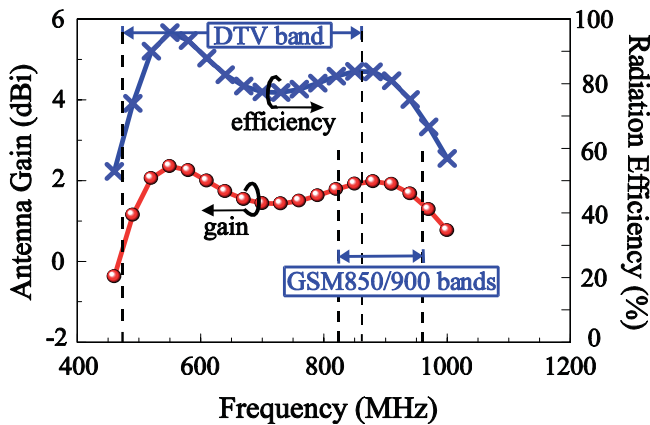


**Figure 9** Measured antenna gain and simulated radiation efficiency for the proposed antenna. [Color figure can be viewed in the online issue, which is available at [www.interscience.wiley.com](http://www.interscience.wiley.com)]

which is generally accepted for DTV reception and mobile communications in the mobile devices, the operating band covers DTV and GSM850/900 operations.

Figure 3 shows the measured return loss for the proposed antenna and the corresponding conventional planar dipole antenna (see insets in the figure). It is clearly seen that there is only one resonant mode (half-wavelength mode) excited at about 570 MHz for the conventional antenna, and the obtained bandwidth is much smaller than that of the proposed antenna. In addition, the fundamental resonant frequency of the proposed antenna is less than that of the conventional antenna; that is, the proposed antenna can have a reduced length as compared to the conventional antenna for covering DTV/GSM operation in this study. This behavior also agrees with the discussion in Section 2.

Figures 4(a) and 4(b) shows the simulated excited surface current distributions at 550 and 900 MHz for the proposed antenna, while Figure 4(c) shows the surface current distributions at 900 MHz for the corresponding conventional planar dipole antenna. Results clearly indicate that the one-wavelength mode of the conventional antenna is not excited. For the proposed antenna, however, good excitation of the half- and one-wavelength modes is seen.

Effects of the dimensions of the tuning slot are also studied. The measured return loss as a function of the length  $L$  is shown in Figure 5. The width  $W$  of the tuning slot is fixed as 10 mm in this study. Note that the length ( $L + 1$  mm) of the tuning strip is varied as the length ( $L$ ) of the tuning slot is varied. When the length  $L$  is increased to be 31 or 47 mm, good excitation of the one-wavelength mode is seen. Both the half- and one-wavelength modes are also shifted to lower frequencies with an increase in  $L$ . However, there exists an optimal length  $L$  to achieve a wider bandwidth formed by the half- and one-wavelength modes with 3:1 VSWR to cover the desired DTV and GSM850/900 bands. In this study, the optimal length  $L$  is determined to be 31 mm as shown in the figure.

Results of the width  $W$  varied from 0 to 12 mm for the length  $L$  fixed as 31 mm are shown in Figure 6. In this case, it is first seen that good excitation of the one-wavelength mode cannot be obtained when the tuning slot is not present ( $W = 0$ ). With the presence of the tuning slot, the impedance matching of the one-wavelength mode is quickly improved. When the width  $W$  is chosen to be 10 mm, good impedance matching of the proposed antenna for covering the desired DTV/GSM operation is obtained.

The radiation characteristics are also studied. Figures 7 and 8 plot the measured radiation patterns at 550 and 900 MHz, respec-

tively. From the results, similar dipole like radiation patterns at 550 and 900 MHz are obtained. Similar radiation patterns for other frequencies over the desired DTV and GSM850/900 bands have also been observed. These radiation patterns are not shown here for brevity. Figure 9 shows the measured antenna gain and simulated radiation efficiency for the proposed antenna. Over the DTV band of 470 ~ 862 MHz, the antenna gain is varied from about 0.2 to 2.2 dBi, and the radiation efficiency is generally larger than 60%. For the GSM850/900 band, the antenna gain is varied from about 1.4 to 2.0 dBi, and the radiation efficiency is larger than about 68%.

#### 4. CONCLUSION

A novel broadband planar dipole antenna showing a very wide operating band for covering DTV signal reception in the 470 ~ 862 MHz band and GSM850/900 operation in the 824 ~ 894/890 ~ 960 MHz band has been proposed, fabricated, and tested. The planar dipole antenna not only is easy to fabricate, but also provides a very wide operating band to cover DTV/GSM operation. The obtained operating bandwidth is generally larger than those of the reported planar DTV antennas for mobile devices [1-5, 11-14], and the broadband operation is achieved from successful excitation of the half- and one-wavelength modes of the proposed planar dipole antenna. Over the operating band of the antenna, good radiation characteristics for DTV/GSM operation have also been obtained. The proposed antenna is especially suitable to be attached on the window pane of a vehicle for practical applications.

#### REFERENCES

1. Y.W. Chi, K.L. Wong, and S.W. Su, Broadband printed dipole antenna with a step-shaped feed gap for DTV signal reception, *IEEE Trans Antennas Propagat* 55 (2007), 3353-3356.
2. Y.W. Chi, K.L. Wong, and S.H. Yeh, End-fed modified planar dipole antenna for DTV signal reception, *Microwave Opt Technol Lett* 49 (2007), 676-680.
3. H. Iizuka, T. Watanabe, K. Sakakibara, and N. Nikuma, Stub-loaded folded dipole antenna for digital terrestrial TV reception, *IEEE Antennas Propagat Lett* 5 (2006), 260-261.
4. S. Matsuzawa, K. Sato, and K. Nishikawa, Study of on-glass mobile antennas for digital terrestrial television, *IEICE Trans Commun E88-B* (2005), 3094-3096.
5. H. Iizuka, T. Watanabe, K. Sato, and K. Nishikawa, Modified H-shaped antenna for automotive digital terrestrial reception, *IEEE Trans Antennas Propagat* 53 (2005), 2542-2548.
6. G. Faria, J.A. Henriksson, E. Stare, and P. Talmola, DVB-H: Digital broadcast services to handheld devices, *Proc IEEE* 94 (2006), 194-209.
7. <http://www.ntia.doc.gov/osmhome/allochrt.html>, U.S. Frequency Allocations, Office of Spectrum Management, National Telecommunications and Information Administration, U.S.A.
8. K.L. Wong, *Planar antennas for wireless communications*, Wiley, New York, 2003.
9. C.M. Su, H.T. Chen, and K.L. Wong, Printed dual-band dipole antenna with U-slotted arms for 2.4/5.2 GHz WLAN operation, *Electron Lett* 38 (2002), 1308-1309.
10. C.Y. Fang, C.M. Su, T.W. Chiou, and K.L. Wong, Dual-band dipole antenna, U.S. Patent No. 6,621,464 B1, Sep. 16, 2003.
11. J.N. Lee, J.K. Park, and B.J. Yim, Design of the novel DVB-H antenna for mobile handset terminal, *Microwave Opt Technol Lett* 49 (2007), 2345-2350.
12. W.Y. Li, K.L. Wong, and J.S. Row, Broadband planar shorted monopole antenna for DTV signal reception in a portable media player, *Microwave Opt Technol Lett* 49 (2007), 558-561.
13. W.Y. Li, K.L. Wong, and S.W. Su, Broadband integrated DTV antenna for USB dongle application, *Microwave Opt Technol Lett* 49 (2007), 1018-1021.

14. K.L. Wong, Y.W. Chi, B. Chen, and S. Yang, Internal DTV antenna for folder-type mobile phone, *Microwave Opt Technol Lett* 48 (2006), 1015-1019.
15. <http://www.ansoft.com/products/hf/hfss/>, Ansoft Corporation HFSS.

© 2008 Wiley Periodicals, Inc.

## A LOW-VOLTAGE DIVIDE-BY-3 INJECTION-LOCKED FREQUENCY DIVIDER

Chien-Feng Lee and Sheng-Lyang Jang

Department of Electronic Engineering, National Taiwan University of Science and Technology, 43 Keelung Road, Section 4, Taipei, Taiwan 106, Republic of China; Corresponding author: D9202209@mail.ntust.edu.tw

Received 13 November 2007

**ABSTRACT:** This study proposes a new low-voltage divide-by-3 CMOS injection locked frequency divider (ILFD) fabricated in a 0.18- $\mu\text{m}$  CMOS process and describes the operation principle of the ILFD. The ILFD circuit is realized with a CMOS dynamic threshold voltage LC-tank voltage-controlled-oscillator (VCO) with two injection MOSFETs. The self-oscillating VCO is injection-locked by third-harmonic input to obtain the division order of three. Measurement results show that at the supply voltage of 0.36 V, the free-running frequency is from 1.015 to 1.093 GHz. At the incident power of  $-10$  dBm, the locking range is from the incident frequency 3.01 to 3.33 GHz. This is the lowest voltage ILFD ever reported in literatures. © 2008 Wiley Periodicals, Inc. *Microwave Opt Technol Lett* 50: 1905–1908, 2008; Published online in Wiley InterScience (www.interscience.wiley.com). DOI 10.1002/mop.23499

**Key words:** divide-by-3; low voltage; injection-locked frequency divider; CMOS; LC-tank VCO; transformer

### 1. INTRODUCTION

The increasing demands on portable wireless devices have motivated the development of CMOS radio frequency integrated circuits (RFICs). These portable devices require low power dissipation to maximize battery lifetime. Some low power applications, such as wireless medical telemetry, require the portable devices to operate at a low supply voltage with a small battery or environment energy, so the power and supply voltage constriction is a key issue for these designs [1].

Frequency dividers (FDs) are widely used for sub-blocks of phase locked loop (PLL) and carrier recovery blocks. The design of a fully integrated CMOS divider is critical for its power con-

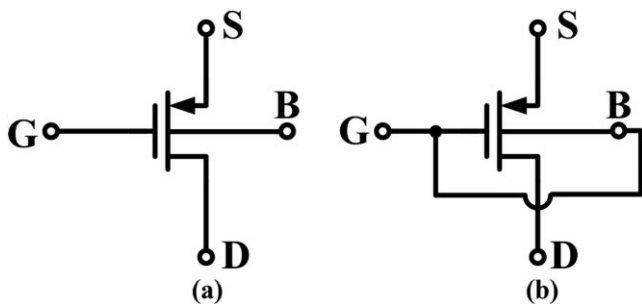


**Figure 1** Configurations on the basis of a pMOS for (a) standard MOS-FET and for (b) dynamic threshold voltage MOS (DTMOS)

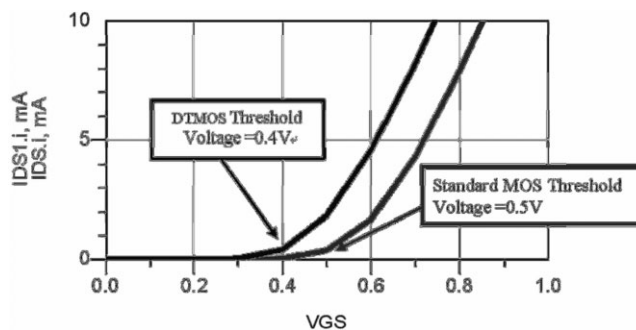


**Figure 2** Simulated current-to-voltage characteristics for both DTMOS and standard MOS configurations

sumption that is comparable with that of the voltage controlled oscillator (VCO). One popular FD is the divide-by-2 LC-tank injection-locked frequency divider (ILFD) [1], which has been well studied, while the divide-by-3 LC ILFD has received much less attention. In the past, only a few experimental results have been published about the divide-by-3 ILFDs [2-4], which were not designed for low voltage operation.

In this study, we propose a new low-voltage divide-by-three LC tank frequency divider, the divide-by-three ILFD is designed using the dynamic threshold voltage MOSFET (DTMOS) VCO as the ILFD core [5]. The low voltage divide-by-three ILFD circuit proposed here was fabricated in a 0.18- $\mu\text{m}$  CMOS process. At the incident power of  $-10$  dBm, the locking range is from 3.01 to 3.33 GHz. This article is organized as follows. Section 2 discusses the operation principle of circuit. Section 3 is the experimental result. Finally, a conclusion is drawn.

### 2. CIRCUIT DESIGN

The operation principle of DTMOS can be seen from Figures 1 and 2. Figure 1(a) shows a standard pMOS transistor and Figure 1(b) shows a DTMOS with gate and substrate contacts connected together. Figure 2 shows the simulated current-to-voltage characteristics for both DTMOS configuration and conventional MOS configuration. The standard MOS has the threshold voltage around 600 mV, while the DTMOST configuration has the threshold voltage about 350–450 mV as shown in Figure 2.

The circuit diagram of the proposed circuit is shown in Figure 3, which consists of a DTMOS LC VCO [5] with two injection MOSFETs (M3 and M4). The voltage  $v_{\text{tune}}$  is used to tune the capacitance of varactors and the oscillation frequency. The injection signal is applied to the gates of M3 and M4 with dc gate bias

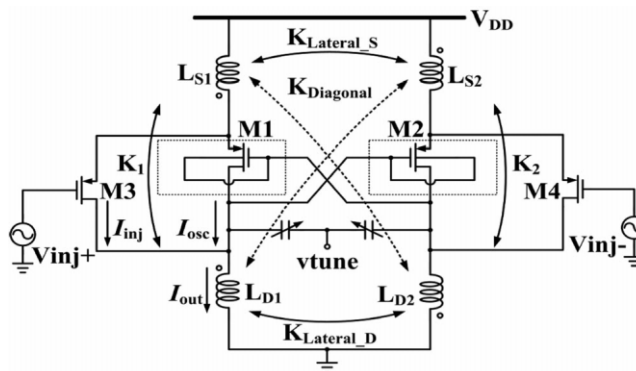


**Figure 3** The proposed low-voltage divide-by-3 ILFD